

Evolution of Eu^{2+} spin dynamics in $\text{Ba}_{1-x}\text{Eu}_x\text{Fe}_2\text{As}_2$ P. F. S. Rosa,^{1,2} C. Adriano,^{1,2} W. Iwamoto,¹ T. M. Garitezi,¹ T. Grant,² Z. Fisk,² and P. G. Pagliuso^{1,2}¹*Instituto de Física “Gleb Wataghin,” UNICAMP, Campinas-SP, 13083-859, Brazil*²*University of California, Irvine, California 92697-4574, USA*

(Received 8 June 2012; revised manuscript received 15 October 2012; published 24 October 2012)

Single crystals of $\text{Ba}_{1-x}\text{Eu}_x\text{Fe}_2\text{As}_2$ were studied by magnetic susceptibility, heat capacity, resistivity, and electron spin resonance (ESR) measurements. Spin-density wave (at T_{SDW}) and antiferromagnetic (at T_N) phase transitions were mapped as a function of x . For $x \geq 0.2$, we found a single Eu^{2+} ESR Dysonian line that presents an isotropic linear increase (Korringa) of its linewidth (ΔH) above T_{SDW} which systematically decreases with decreasing x . In contrast, for a critical concentration x_c ($0.10 < x_c < 0.20$), ΔH decreases with increasing T , suggesting a distinct relaxation process that we associate with a Eu^{2+} Kondo single impurity regime. The Korringa rate suppression towards the Ba-rich compounds is claimed to be due to the reduction of the q -dependent exchange interaction between the Eu^{2+} f electrons and the conduction electrons, which is likely associated with an increasing of localization of Fe d electrons. This result may help the understanding of the SDW phase suppression (that can lead to superconductivity) in this class of materials.

DOI: [10.1103/PhysRevB.86.165131](https://doi.org/10.1103/PhysRevB.86.165131)

PACS number(s): 71.27.+a, 74.70.Xa, 76.30.-v

I. INTRODUCTION

The Fe-based superconductors $R\text{FeAsO}$ ($R = \text{La-Gd}$) and $A\text{Fe}_2\text{As}_2$ ($A = \text{Ba, Sr, Ca, Eu}$) have been a topic of intense scientific investigation since their discovery.^{1,2} Particularly interesting is the fact that superconductivity (SC) can be found in both FeAs-based systems with comparable critical temperatures despite the fact that one class is an oxide family and the other is an intermetallic system.³ The latter crystallizes in the tetragonal ThCr_2Si_2 -type structure ($I4/mmm$) and exhibits a structural distortion accompanied by a spin-density wave (SDW) phase transition ($100 \text{ K} \lesssim T_{\text{SDW}} \lesssim 200 \text{ K}$). It is remarkable that this SDW phase can be tuned towards a SC state by doping and applied pressure. However, a microscopic understanding of the interplay between SDW and SC is still an open question that strongly motivates further research on these materials. In this regard, microscopic spin probes that can directly study the spin dynamics of SDW and SC phases are highly desirable.

Electron spin resonance (ESR) is a powerful spin probe that has been used to study the spin dynamics in these compounds. However, up to date, the ESR experiments have been focused on Eu-based samples far from the diluted regime. For instance, Eu^{2+} ESR data in EuFe_2As_2 single crystals indicate a spatial confinement of the conduction electrons (ce) to the FeAs layers below T_{SDW} due to the change in the ESR linewidth from a typical metallic behavior (i.e., a linear Korringa-type increase⁴) above T_{SDW} to a magnetic insulating behavior, where dipolar and crystalline electrical field effects dominate.⁵ In hole doped $\text{Eu}_{0.5}\text{K}_{0.5}\text{Fe}_2\text{As}_2$, where the SDW phase is completely suppressed and SC arises for $T \leq 32 \text{ K}$, a Korringa increase also occurs for $T > T_c$.⁶ For the electron doped $\text{EuFe}_{2-x}\text{Co}_x\text{As}_2$, the Korringa rate (KR), T_{SDW} , and T_c scale with x .⁷ A recent report on polycrystalline $\text{EuFe}_{2-x}\text{Co}_x\text{As}_2$ also shows a KR decreasing with Co doping.⁸ However, in the Eu-concentrated compounds, the Eu^{2+} - Eu^{2+} spin interaction always represents an important contribution to the ESR data and to the global properties of the compounds. Therefore, it is crucial to extrapolate such studies to a Eu^{2+} diluted regime in a host compound of great interest. BaFe_2As_2

is an obvious choice since it presents $T_{\text{SDW}} = 140 \text{ K}$ and SC can be tuned by pressure and doping. In fact, the highest SC T_c within the $A\text{Fe}_2\text{As}_2$ series is found in $(\text{Ba, K})\text{Fe}_2\text{As}_2$ (38 K).^{9,10}

II. EXPERIMENTAL DETAILS

We report a systematic study of flux grown $\text{Ba}_{1-x}\text{Eu}_x\text{Fe}_2\text{As}_2$ ($x_{\text{nominal}} = 0.01, 0.1, 0.2, 0.3, 0.5, 0.7, 0.9, 1.0$) by means of magnetic susceptibility, heat capacity, resistivity, and ESR experiments. To increase signal to noise ratio, mainly larger Sn-flux crystals were used in the ESR experiments.¹¹ Selected concentrations were also grown from In and self(FeAs)-fluxes.^{12,13} The crystals were checked by x-ray powder diffraction and submitted to elemental analysis using a commercial energy dispersive spectroscopy (EDS) microprobe. As previously reported, the Sn-flux crystals were found to have a small amount of Sn incorporation varying from 0.1 to 1.0 at. % along the series.¹⁴ No In incorporation was detected in the In-flux crystals. From the EDS analysis we also extracted the actual Eu- x that are used throughout the text. The in-plane resistivity was measured using a four-probe method. Specific heat data were taken in a commercial small-mass calorimeter and the magnetization data was collected using a superconducting quantum interference device (SQUID) magnetometer. X-band ($\nu = 9.34 \text{ GHz}$) ESR measurements were performed in a commercial spectrometer with a continuous He gas-flow cryostat.

III. RESULTS AND DISCUSSION

To better illustrate the evolution of the physical properties along the series, we present the data of four representative Eu concentrations. Figure 1(a) displays the T dependence of the specific heat per mole divided by temperature. For $x = 0.95$, two sharp peaks indicate both SDW and AFM transitions at 187 and 18 K, respectively, which are slightly down-shifted when compared to 189 and 19 K in EuFe_2As_2 . As x decreases, T_N is further suppressed and the lowest detectable $T_N = 0.5 \text{ K}$ is obtained for $x = 0.55$ (inset). Interestingly, even for $x < 0.5$,

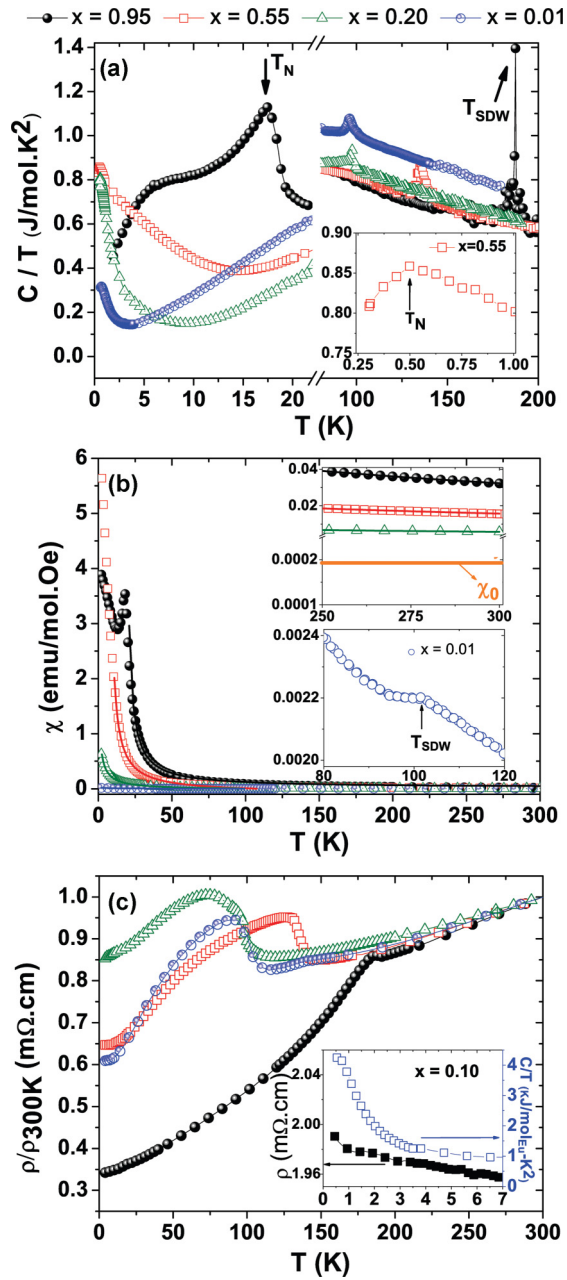


FIG. 1. (Color online) Physical properties of $\text{Ba}_{1-x}\text{Eu}_x\text{Fe}_2\text{As}_2$. The inset shows (a) low- T data for $x = 0.55$, (b) high- T data and T_{SDW} for $x = 0.01$, and (c) low- T data upturn for $x = 0.10$.

where the AFM is no longer present, we observed a rise in C/T at low- T which is not found for $x = 0$, indicating that the Eu^{2+} ions are responsible for it.

Figure 1(b) shows the magnetic susceptibility as a function of temperature for $H = 1$ kOe parallel to the ab plane. For all samples, $\chi(T)$ can be fitted to a Curie-Weiss law plus a T -independent Pauli term, $\chi(T) = \chi_0 + C/(T - \theta_{\text{CW}})$ (solid lines). We obtained $\chi_0 = 2(1) \times 10^{-3}$ emu/molOe [upper inset of Fig. 1(b)] and an effective moment $\mu_{\text{eff}} \approx 8\mu_B$ for Eu^{2+} ions for all x values. The SDW transition is nearly undistinguishable in the Eu-rich samples due to the Eu^{2+} large magnetic contribution but it can be seen as a kink in $\chi(T)$ for samples in the Eu-diluted regime [bottom inset of Fig. 1(b)].

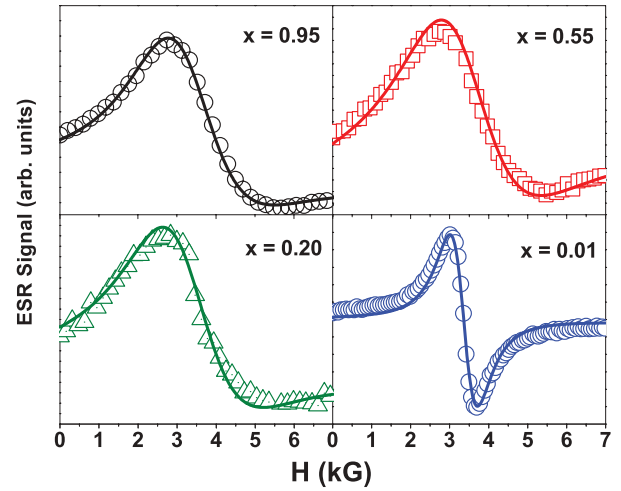


FIG. 2. (Color online) X-band spectra at $T = 300$ K for $H \parallel ab$.

The T dependence of the normalized electrical resistivity is shown in Fig. 1(c). The room- T value of $\rho(T)$ and RRR ratio varies in the range 0.2–0.8 m Ω cm and 0.02–2.8, respectively. For $x > 0.5$, a metallic behavior is observed down to T_{SDW} where a sudden drop can be identified in the curves. For $x \lesssim 0.5$, $\rho(T)$ increases at T_{SDW} as typically found for doped samples in the BaFe_2As_2 systems.³

Figure 2 shows the X-band ESR spectra at $T = 300$ K and $H \parallel ab$ for $\text{Ba}_{1-x}\text{Eu}_x\text{Fe}_2\text{As}_2$ single crystals. A single Eu^{2+} ESR resonance is observed for all x values. The ESR lines for $x \geq 0.2$ have an asymmetric Dysonian character (skin depth smaller than the sample size¹⁵). However, for $x < 0.2$, the spectra clearly becomes more symmetric, consistent with the fact that BaFe_2As_2 has smaller conductivity than EuFe_2As_2 . In addition, it is evident that the ESR linewidth (ΔH) is much smaller in the Eu-diluted regime, consistent with the decreasing of the Eu^{2+} - Eu^{2+} spin interaction contribution to the ESR ΔH .

From fitting to the resonances using the appropriate admixture of absorption and dispersion (solid lines), we obtained both ΔH and g -value T dependence, shown in Fig. 3. In the Eu-rich extreme, we observe an isotropic linear (Korringa-type) increase of the ΔH with increasing- T for $T > T_{\text{SDW}}$. From linear fits to the $\Delta H(T)$ for $T > T_{\text{SDW}}$ and $x \geq 0.2$ we extracted the values of the KR $b = \Delta H/\Delta T$. It is evident that b systematically decreases with decreasing x along the series for $x \geq 0.2$. Consistently, the $b = 6.3(5)$ Oe/K found for the $x = 0.95$ sample is slightly smaller than the reported $b = 6.5$ – 8.0 Oe/K values for EuFe_2As_2 .^{5,7}

However, for $x < 0.2$ we observe no Korringa behavior. Instead, $\Delta H(T)$ decreases with increasing T , suggesting a nontrivial regime clearly distinct from a Fermi liquid. For $x = 0.01$ we show in Fig. 3(a) that this intriguing behavior was found for crystals grown from different fluxes.

Figure 3(b) displays the T dependence of the Eu^{2+} ESR g -value for $T > 200$ K and $H \parallel ab$. As the crystals are very thin platelets, we use the data for $H \parallel ab$ that allow us to neglect the demagnetization factors to determine the g -values.¹⁶ As previously reported for EuFe_2As_2 , $\text{Eu}_{0.5}\text{Co}_{0.5}\text{Fe}_2\text{As}_2$, and $\text{EuFe}_{2-x}\text{Co}_x\text{As}_2$, we found a T -independent $g \approx 2$ for the

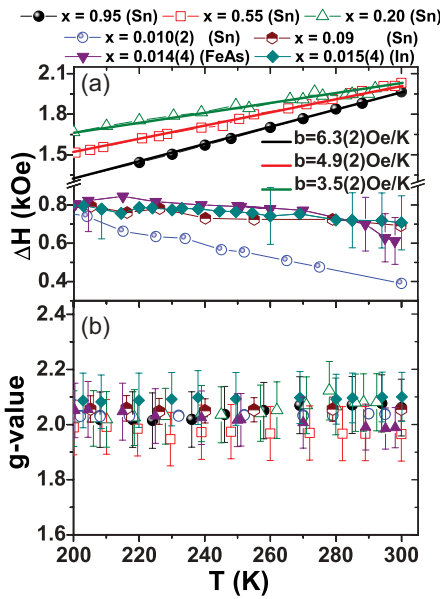


FIG. 3. (Color online) T dependence of the (a) linewidth ΔH and (b) g -value. The data for $x = 0.01$ (In) and $x = 0.01$ (FeAs) were taken in powdered crystals and several small crystals, respectively.

Eu^{2+} ESR lines in $\text{Ba}_{1-x}\text{Eu}_x\text{Fe}_2\text{As}_2$ for $T > T_{\text{SDW}}$. In fact, the high- T Eu^{2+} g -values are also independent of x . For the samples with narrower ESR ΔH ($x < 0.20$) we were able to determine with higher precision a g -value of 2.04(2). This is a more accurate g -value than those published for the concentrated compounds, which possess a much broader ΔH . As it can be seen in Fig. 3(b), the g -value of 2.04(2) is a reasonable mean g -value for all x in this T range. However, although this is a reasonable approximation it must be taken cautiously due to the limitations in our analysis for the broader lines.

From the data in Figs. 1–3, we extracted the phase diagram in Fig. 4. Both T_{SDW} and T_N decrease with $1-x$ and for $x < 0.5$ the Eu^{2+} AFM transition is no longer observable. Interestingly, the decreasing KR follows qualitatively the suppression of T_{SDW} before it disappears at $0.10 < x_c < 0.20$.

To gain a microscopic understanding of this evolution, a detailed analysis of the ESR data is needed. We consider the simplest scenario for the treatment of the exchange interaction, $J_{fs}\mathbf{S}\cdot\mathbf{s}$, between a localized Eu^{2+} $4f$ electron

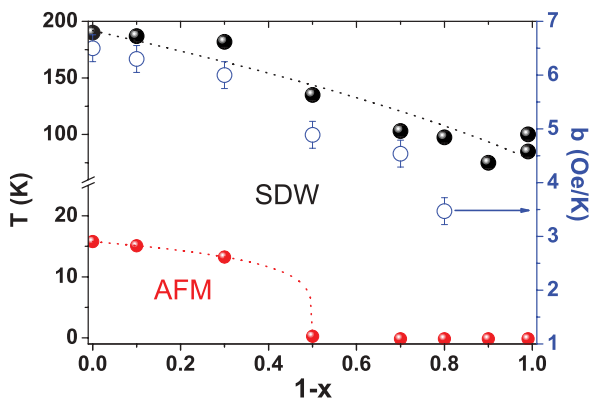


FIG. 4. (Color online) $\text{Ba}_{1-x}\text{Eu}_x\text{Fe}_2\text{As}_2$ phase diagram.

spin (\mathbf{S}) and the free ce spins (\mathbf{s}) of the host metal, where “bottleneck”, “dynamic”, electron-electron correlation effects, \mathbf{q} -dependence exchange, and multiple bands effects are not present.¹⁷ Those are reasonable assumptions because when “dynamic” effects are present the g -values are usually strongly T dependent and when the bottleneck effect is relevant the KR decreases with the increasing of the concentration of the magnetic ions.¹⁷ None of these effects are observable in our ESR data of Fig. 3 in the studied T range.

Therefore, in this simple case, the ESR g -shift (Knight shift)¹⁸ and the Korringa rate¹⁹ can be written as

$$\Delta g = J_{fs}\eta(E_F) \quad (1)$$

and

$$\frac{d(\Delta H)}{dT} = \frac{\pi k}{g\mu_B} J_{fs}^2 \eta^2(E_F), \quad (2)$$

where J_{fs} is the effective exchange interaction between the Eu^{2+} local moment and the ce in the absence of ce momentum transfer,²⁰ $\eta(E_F)$ the “bare” density of states (DOS) for one spin direction at the Fermi surface (FS), k the Boltzman constant, μ_B the Bohr magneton, and g the Eu^{2+} g -value. When Eqs. (1) and (2) are applicable, the relation $\frac{d(\Delta H)}{dT} = \frac{\pi k}{g\mu_B} (\Delta g)^2$ holds. Using the g -value of Eu^{2+} in insulators as 1.993(2), $(\pi k/g\mu_B) = 2.34 \times 10^4$ Oe/K and replacing $\Delta g \approx 0.05(2)$, we found a $b \approx 150(50)$ Oe/K for the Eu^{2+} resonance.²¹

That value is much larger than the measured values of b for $x \geq 0.20$ (see Figs. 3 and 4). Therefore, the approximations made in Eqs. (1) and (2) are not valid for these compounds and we have to consider a \mathbf{q} -dependent exchange interaction, $J_{fs}(\mathbf{q})$, and perhaps conduction electron-electron ($e-e$) correlations.^{22,23} $J_{fs}(\mathbf{q})$ is the Fourier transform of the spatially varying exchange.

Considering only the wave-vector dependence of the exchange interaction, $J_{fs}(\mathbf{q})$, the exchange parameters in Eqs. (1) and (2) become $J_{fs}(\mathbf{0})$ and $\langle J_{fs}^2(\mathbf{q}) \rangle$, respectively. At the Eu^{2+} site the g shift probes the ce polarization ($\mathbf{q} = 0$) and the Korringa rate the ce momentum transfer ($0 \leq \mathbf{q} \leq 2k_F$) averaged over the FS.²⁰

To evaluate the possible contribution of $e-e$ correlations in our ESR data, we need to estimate the Pauli magnetic susceptibility.^{22,23} The electronic contribution to the heat capacity for the BaFe_2As_2 compound is reported to be $\gamma = 16$ mJ/molK².² Assuming a free ce gas model for BaFe_2As_2 , $\gamma = (2/3)\pi k^2 \eta(E_F)$, we calculate a DOS at the Fermi level (E_F), $\eta(E_F) = 3.34$ states/eV mol spin. Then, one finds an electronic spin susceptibility, $\chi_e = 2\mu_B^2 \eta(E_F)$, of $\approx 3 \times 10^{-4}$ emu/FU. That is one order smaller than the $\chi_0 = 2(1) \times 10^{-3}$ emu/mol Oe measured for all compounds (Fig. 1). This suggests that an $e-e$ exchange enhancement contributes to the ce spin susceptibility in $\text{Ba}_{1-x}\text{Eu}_x\text{Fe}_2\text{As}_2$. It is known that, in the presence of such an enhancement, the host metal ce spin susceptibility can be approximated by $\chi_0 = 2\mu_B^2 \frac{\eta(E_F)}{1-\alpha}$, where α accounts for the $e-e$ interaction, $(1-\alpha)^{-1}$ is the Stoner enhancement factor, and $\eta(E_F)$ the “bare” DOS for one spin direction at E_F .^{22,23} An α value of $\approx 0.85(5)$ is estimated assuming that the enhancement in χ_0 is only due to the $e-e$ interaction.

In the presence of e - e exchange enhancement and a \mathbf{q} dependence of the exchange interaction, $J_{fs}(\mathbf{q})$, the g shift [Eq. (1)] and the thermal broadening of the linewidth [Eq. (2)] may be rewritten as

$$\Delta g = J_{fs}(\mathbf{0}) \frac{\eta(E_F)}{1 - \alpha} \quad (3)$$

and

$$\frac{d(\Delta H)}{dT} = \frac{\pi k}{g\mu_B} \langle J_{fs}^2(\mathbf{q}) \rangle \eta^2(E_F) \frac{K(\alpha)}{(1 - \alpha)^2}, \quad (4)$$

where $K(\alpha)$ is the Korringa exchange enhancement factor.^{24,25} From Ref. 25, $\alpha \approx 0.85(5)$ corresponds to $K(\alpha) = 0.2(1)$. Then, using $\eta(E_F) = 3.34$ states/eV mol spin, $\Delta g = 0.05(2)$, $\alpha \approx 0.9$, $K(\alpha) = 0.2(1)$, and b values, we extracted $J_{fs}(0) = 2(1)$ meV for all x values and $[\langle J_{fs}^2(\mathbf{q}) \rangle]^{1/2} = 2.0(8), 1.5(8), 1.0(8)$ for $x = 0.95, 0.55, 0.20$, respectively.

It is evident that the relative value of $\langle J_{fs}^2(\mathbf{q}) \rangle^{1/2}$ is clearly diminishing with decreasing x for $\text{Ba}_{1-x}\text{Eu}_x\text{Fe}_2\text{As}_2$ for $x \geq 0.20$ even though we have a large uncertainty in its exact numerical value. $J_{fs}(q)$ is the Fourier transform of the spatially varying exchange and therefore its decreasing value suggests that the electron bands with appreciable overlap with the Eu^{2+} $4f$ states are becoming more anisotropic (less s -like) and are, in average, further away from the Eu^{2+} sites in real space. We speculate that this behavior may be associated to a partial localization of the itinerant Fe d at the Fe sites.

This scenario is consistent with the decrease of T_{SDW} in $\text{Ba}_{1-x}\text{Eu}_x\text{Fe}_2\text{As}_2$. The SDW state in these materials is believed to be associated with itinerant Fe d bands.^{3,26,27} As such, the increase in the d -band localized character may suppress the itinerant SDW state. Similar effects may also be expected in the case of other dopings in the 122 compounds where the SDW suppression leads to SC. Interestingly, data on the concentrated regime have shown a slower KR when K or Co are introduced in EuFe_2As_2 .⁶⁻⁸ Also, band structure calculations and angle resolved photoemission spectroscopy (ARPES) experiments for BaFe_2As_2 and EuFe_2As_2 have shown that there are differences in the FS topology between the two compounds even though the Fe $3d$ DOS are nearly the same close to E_F .^{28,29} ARPES experiments show that the size of the hole pockets near Γ in EuFe_2As_2 is 2–3 times larger than in BaFe_2As_2 , in agreement with the fact that the hole carrier mobility dominates in EuFe_2As_2 as compared to BaFe_2As_2 in the paramagnetic phase.³⁰ Besides, local-density approximation (LDA) calculations show that for slightly smaller Fe-As distances there is a down-shift of the Fe $3d_{x^2-y^2}$ band near Γ leading to a suppression of the Fe magnetism. These FS changes may be reflected in the evolution of $J_{fs}(\mathbf{q})$ with x . Ongoing experiments on Eu-diluted $\text{Ba}_{1-x}\text{Eu}_x\text{Fe}_{2-y}\text{M}_y\text{As}_2$ ($M = \text{Co}, \text{Ru}, \text{Cu},$ and Mn) may help confirm such a scenario. Recent ESR experiments in EuIn_2As_2 report no Korringa behavior, confirming that the Eu^{2+} KR observed in the FeAs-based compounds is due to the coupling between Eu^{2+} $4f$ and Fe $3d$ states.³¹

It is important to mention that, as Eu^{2+} and Ba^{2+} have the same valence, this evolution of the electronic structure is presumably caused by the subtle changes in the tetragonal crystal structures (and in the Fe-As bonds) of EuFe_2As_2 ($c/a = 3.1006$) and BaFe_2As_2 ($c/a = 3.2849$).³² Recent EXAFS experiments reported that the Fe-As bonds in BaFe_2As_2 are slightly smaller upon hydrostatic pressure, hole, and electron doping.³³ The increasing localization of the itinerant Fe d at the Fe sites claimed in this work for $\text{Ba}_{1-x}\text{Eu}_x\text{Fe}_2\text{As}_2$ is consistent with all previous experiments mentioned above and may help the understanding of the SDW phase suppression by doping in this class of materials.

Now we turn our attention to the more diluted regime ($x < 0.20$). The observed decreasing of $\langle J_{fs}^2(q) \rangle^{1/2}$ for ($x \geq 0.20$) may suggest that the KR for the Eu^{2+} diluted regime will be very small and the Eu^{2+} ESR ΔH would be T independent in this T interval. However, this mechanism cannot explain the ΔH broadening observed for $T > T_{\text{SDW}}$ in the $x < 0.20$ samples as T is lowered.

We seek a possible explanation for this behavior by further analyzing the low- T $\rho(T)$ and heat capacity data for the samples in the Eu^{2+} low- x regime. The inset of Fig. 1(c) shows such data for the $x = 0.1$ sample. We speculate that the observed behavior is reminiscent of the Kondo single impurity regime with a Kondo temperature $T_K \approx 5$ –10 K. As such, this result suggests that, for $x < 0.20$, any kind of intersite Eu^{2+} - Eu^{2+} short range magnetic correlation disappears leading to the emergence of intrasite only AFM coupling of the Eu^{2+} $4f$ and the ce . In this Kondo-like interaction, the ce tend to screen the localized Eu^{2+} ions leading to faster relaxation and ΔH broadening as T decreases. This effect would become even more dramatic at lower T if the ΔH were not already strongly enhanced by the presence of the SDW phase in all studied samples. Interestingly, the claim for the presence of Kondo single impurity effect interaction for the Eu^{2+} ions in the 122 system has also been made in the case of EuFe_2P_2 .³⁴

IV. CONCLUSIONS

In summary, single crystals of $\text{Ba}_{1-x}\text{Eu}_x\text{Fe}_2\text{As}_2$ were characterized by transport, magnetic susceptibility, heat capacity, and electron spin resonance experiments. We have found a systematic decrease of the KR with decreasing x that was claimed to be associated with the reduction of the q -dependent exchange interaction between the Eu^{2+} f electrons and the ce . This behavior is attributed to the increasing of the degree of localization of Fe d electrons. We also found that the physical properties of Eu^{2+} dilute samples are consistent with a Eu^{2+} Kondo single impurity regime.

ACKNOWLEDGMENTS

This work was supported by FAPESP (in particular Grants No. 2006/60440-0, No. 2009/09247-3, No. 2010/11949-3, No. 2011/01564-0, and No. 2011/23650-5), CNPq, FINEP-Brazil.

¹Y. Kamihara, T. Watanabe, M. Hirano, and H. Hosono, *J. Am. Chem. Soc.* **130**, 3296 (2008).

²M. Rotter, M. Tegel, D. Johrendt, I. Schellenberg, W. Hermes, and R. Pottgen, *Phys. Rev. B* **78**, 020503(R) (2008).

- ³G. R. Stewart, *Rev. Mod. Phys.* **83**, 1589 (2011), and references therein.
- ⁴The Korringa parameter b represents the thermal broadening rate of the ESR line which is proportional to the relaxation rate ($1/T_1$ where T_1 is the spin-lattice relaxation time) of the Eu^{2+} resonating spins through the ce electrons and ultimately to the lattice. See J. Korringa, *Physica* **16**, 601 (1950), and references therein.
- ⁵E. Dengler, J. Deisenhofer, H.-A. Krug von Nidda, S. Khim, J. S. Kim, K. H. Kim, F. Casper, C. Felser, and A. Loidl, *Phys. Rev. B* **81**, 024406 (2010).
- ⁶N. Pascher, J. Deisenhofer, H. A. Krug von Nidda, M. Hemmida, H. S. Jeevan, P. Gegenwart, and A. Loidl, *Phys. Rev. B* **82**, 054525 (2010).
- ⁷J. J. Ying, T. Wu, Q. J. Zheng, Y. He, G. Wu, Q. J. Li, Y. J. Yan, Y. L. Xie, R. H. Liu, X. F. Wang, and X. H. Chen, *Phys. Rev. B* **81**, 052503 (2010).
- ⁸F. A. Garcia, A. Leithe-Jasper, W. Schnelle, M. Nicklas, H. Rosner, and J. Sichelschmidt, *New J. Phys.* **14**, 063005 (2012).
- ⁹M. Rotter, M. Tegel, and D. Johrendt, *Phys. Rev. Lett.* **101**, 107006 (2008).
- ¹⁰C. Zhang, L. Ling, W. Tong, W. Ling, G. Feng, S. Zhang, L. Pi, S. Tan, and Y. Zhang, *J. Appl. Phys.* **109**, 07E124 (2011).
- ¹¹R. R. Urbano, E. L. Green, W. G. Moulton, A. P. Reyes, P. L. Kuhns, E. M. Bittar, C. Adriano, T. M. Garitezi, L. Bufaical, and P. G. Pagliuso, *Phys. Rev. Lett.* **105**, 107001 (2010).
- ¹²T. M. Garitezi *et al.* (unpublished).
- ¹³N. Ni, M. E. Tillman, J.-Q. Yan, A. Kracher, S. T. Hannahs, S. L. Budko, and P. C. Canfield, *Phys. Rev. B* **78**, 214515 (2008).
- ¹⁴Y. Su, P. Link, A. Schneidewind, T. Wolf, P. Adelman, Y. Xiao, M. Meven, R. Mittal, M. Rotter, D. Johrendt, T. Brueckel, and M. Loewenhaupt, *Phys. Rev. B* **79**, 064504 (2009).
- ¹⁵F. J. Dyson, *Phys. Rev.* **98**, 349 (1955).
- ¹⁶R. R. Urbano, P. G. Pagliuso, C. Rettori, A. Malachias, E. Granado, P. Schlottmann, Z. Fisk, and S. B. Oseroff, *Phys. Rev. B* **73**, 115123 (2006).
- ¹⁷C. Rettori, H. M. Kim, E. P. Chock, and D. Davidov, *Phys. Rev. B* **10**, 1826 (1974).
- ¹⁸K. Yosida, *Phys. Rev.* **106**, 893 (1957).
- ¹⁹J. Korringa, *Physica* **16**, 601 (1950).
- ²⁰D. Davidov, K. Maki, R. Orbach, C. Rettori, and E. P. Chock, *Solid State Commun.* **12**, 621 (1973).
- ²¹A. Abragam and B. Bleaney, *EPR of Transition Ions* (Clarendon Press, Oxford, 1970).
- ²²T. Moriya, *J. Phys. Soc. Jpn.* **18**, 516 (1963).
- ²³A. Narath, *Phys. Rev.* **163**, 232 (1967).
- ²⁴A. Narath and H. T. Weaver, *Phys. Rev.* **175**, 373 (1968).
- ²⁵R. W. Shaw and W. W. Warren, *Phys. Rev. B* **3**, 1562 (1971).
- ²⁶I. I. Mazin, D. J. Singh, M. D. Johannes, and M. H. Du, *Phys. Rev. Lett.* **101**, 057003 (2008).
- ²⁷A. V. Chubukov, D. V. Efremov, and I. Eremin, *Phys. Rev. B* **78**, 134512 (2008).
- ²⁸C. Krellner, N. Caroca-Canales, A. Jesche, H. Rosner, A. Ormeci, C. Geibel, and C. Geibel, *Phys. Rev. B* **78**, 100504 (2008).
- ²⁹T. Setti. Ph.D. thesis, Tech. Universitat Berlin, 2011.
- ³⁰Z. Ren, Z. Zhu, S. Jiang, X. Xu, Q. Tao, C. Wang, C. Feng, G. Cao, and Z. Xu, *Phys. Rev. B* **78**, 052501 (2008).
- ³¹P. F. S. Rosa, C. Adriano, T. M. Garitezi, R. A. Ribeiro, Z. Fisk, and P. G. Pagliuso, *Phys. Rev. B* **86**, 094408 (2012).
- ³²U. Alver, R. G. Goodrich, N. Harrison, D. W. Hall, E. C. Palm, T. P. Murphy, S. W. Tozer, P. G. Pagliuso, N. O. Moreno, J. L. Sarrao, and Z. Fisk, *Phys. Rev. B* **64**, 180402(R) (2001).
- ³³E. Granado, L. Mendonca-Ferreira, F. Garcia, G. de M. Azevedo, G. Fabbris, E. M. Bittar, C. Adriano, T. M. Garitezi, P. F. S. Rosa, L. F. Bufaical, M. A. Avila, H. Terashita, and P. G. Pagliuso, *Phys. Rev. B* **83**, 184508 (2011).
- ³⁴C. Feng, Z. Ren, S. Xu, S. Jiang, Z. A. Xu, G. Cao, I. Nowik, I. Felner, K. Matsubayashi, and Y. Uwatoko, *Phys. Rev. B* **82**, 094426 (2010).